

# Vehicle Dynamics

## Synchronous mechanism modeling

Dr. Bóka Gergely

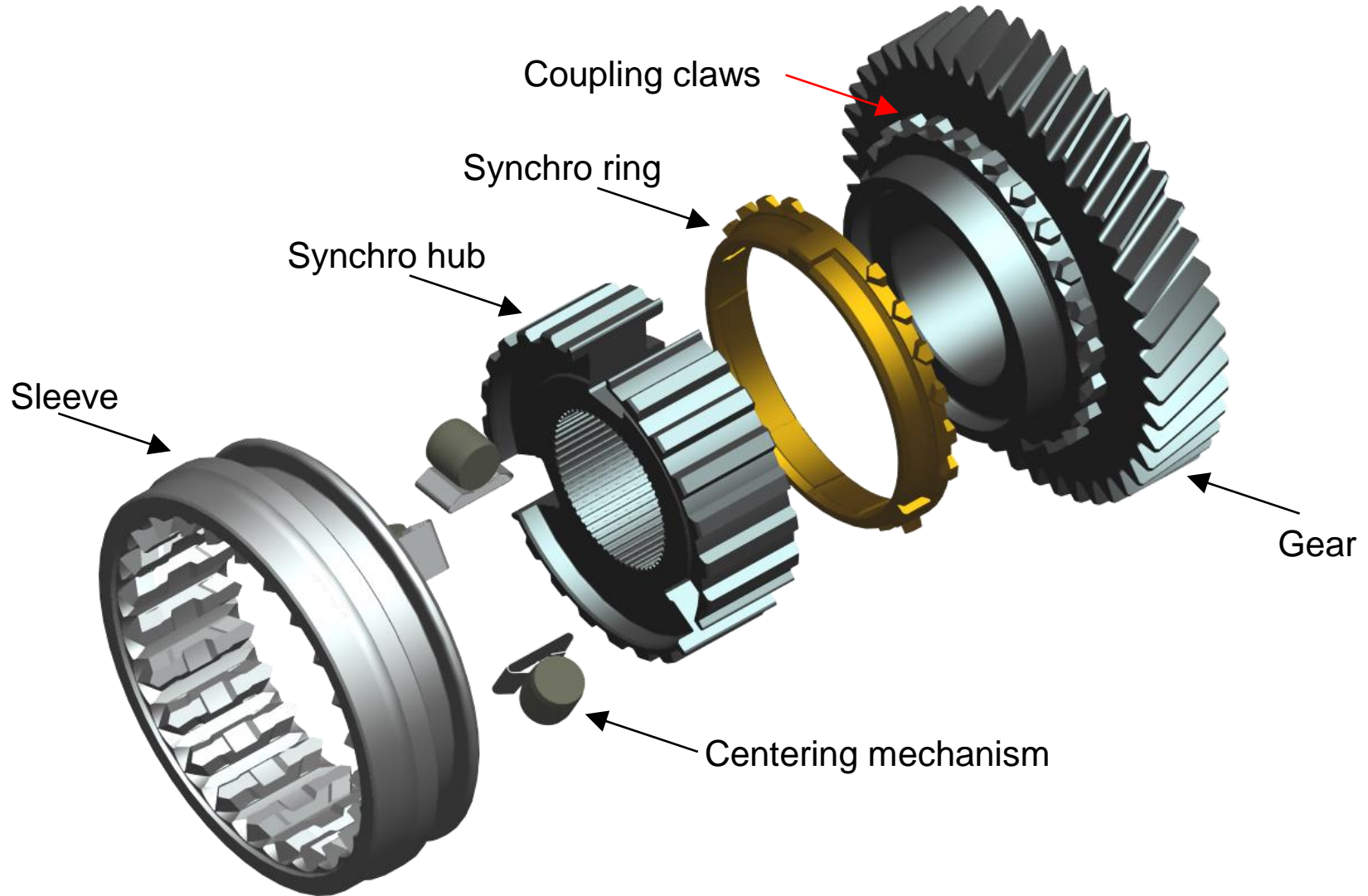
Vass Sándor



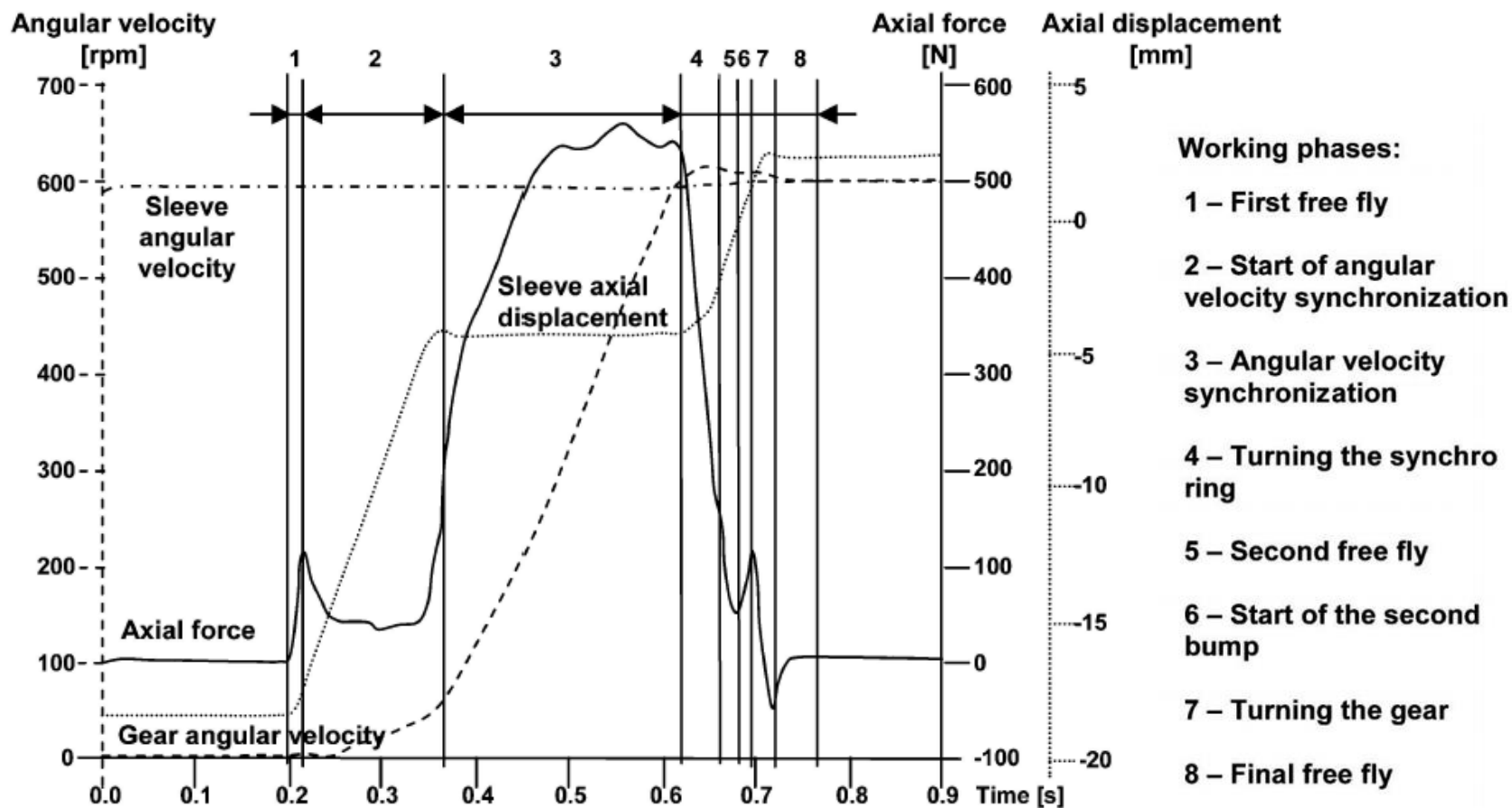
## Contents

- **Buildup of a synchronous mechanism, the synchronization process**
- Stressing of a synchronous mechanism
- State flow chart based synchronous mechanism model

## Buildup of a synchronous mechanism (Borg-Warner type)



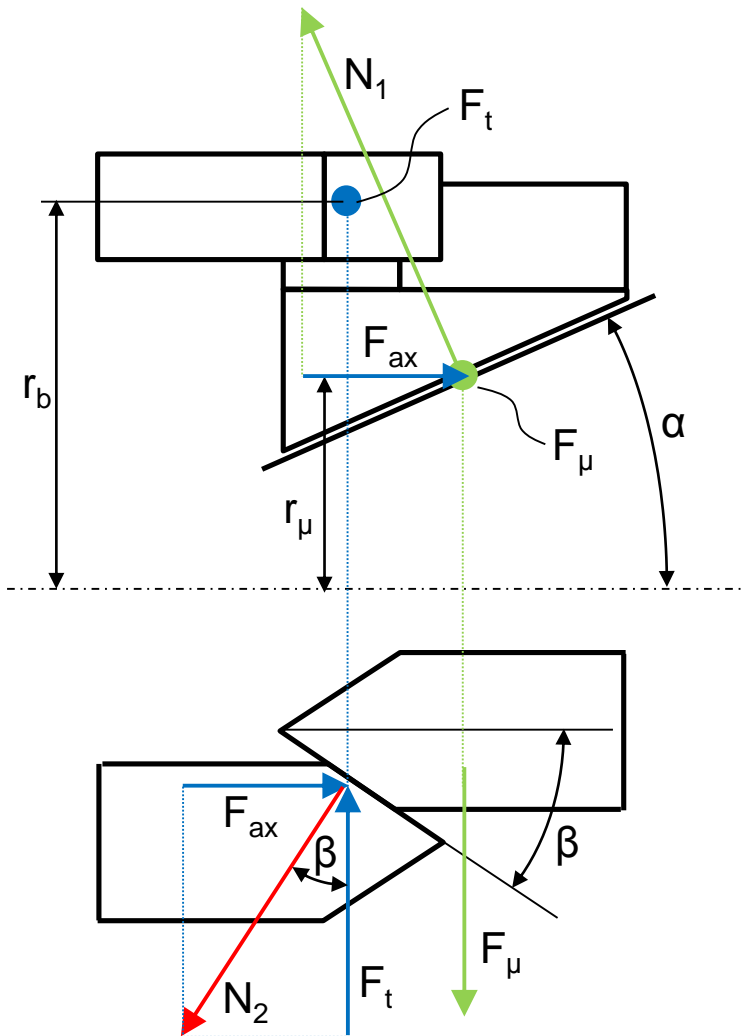
## A szinkronszerkezet kapcsolási folyamat szakaszai [1]



## Contents

- Buildup of a synchronous mechanism, the synchronization process
- **Stressing of a synchronous mechanism**
- State flow chart based synchronous mechanism model

## Designing the locking mechanism (approximate)



Tangential force on the synchronizing cone:

$$F_\mu = \mu N_1 = \mu \frac{F_{ax}}{\sin \alpha}$$

Slipping limit on the coupling claws:

$$\left. \begin{array}{l} F_{ax} = N_2 \sin \beta \\ F_t = N_2 \cos \beta \end{array} \right\} \Rightarrow F_t = \frac{F_{ax}}{\tan \beta}$$

Criterion for coupling/locking:  $M_\mu > M_t$

$$\begin{aligned} r_\mu F_\mu &> r_b F_t \\ r_\mu \mu \frac{F_{ax}}{\sin \alpha} &> r_b \frac{F_{ax}}{\tan \beta} \\ \boxed{\tan \beta} &> \frac{r_b \sin \alpha}{r_\mu \mu} \end{aligned}$$

From locking point of view a blunter claw is preferable, while a sharper claw makes synchronisation process faster. Characteristic values:

$\alpha \approx 6-8^\circ > \arctg(\mu)$ , to avoid self-locking

$\beta \approx 46-64^\circ$ , the least value, which is able to lock

## Contents

- Buildup of a synchronous mechanism, the synchronization process
- Stressing of a synchronous mechanism
- **State flow chart based synchronous mechanism model**

## Model characteristics and assumptions

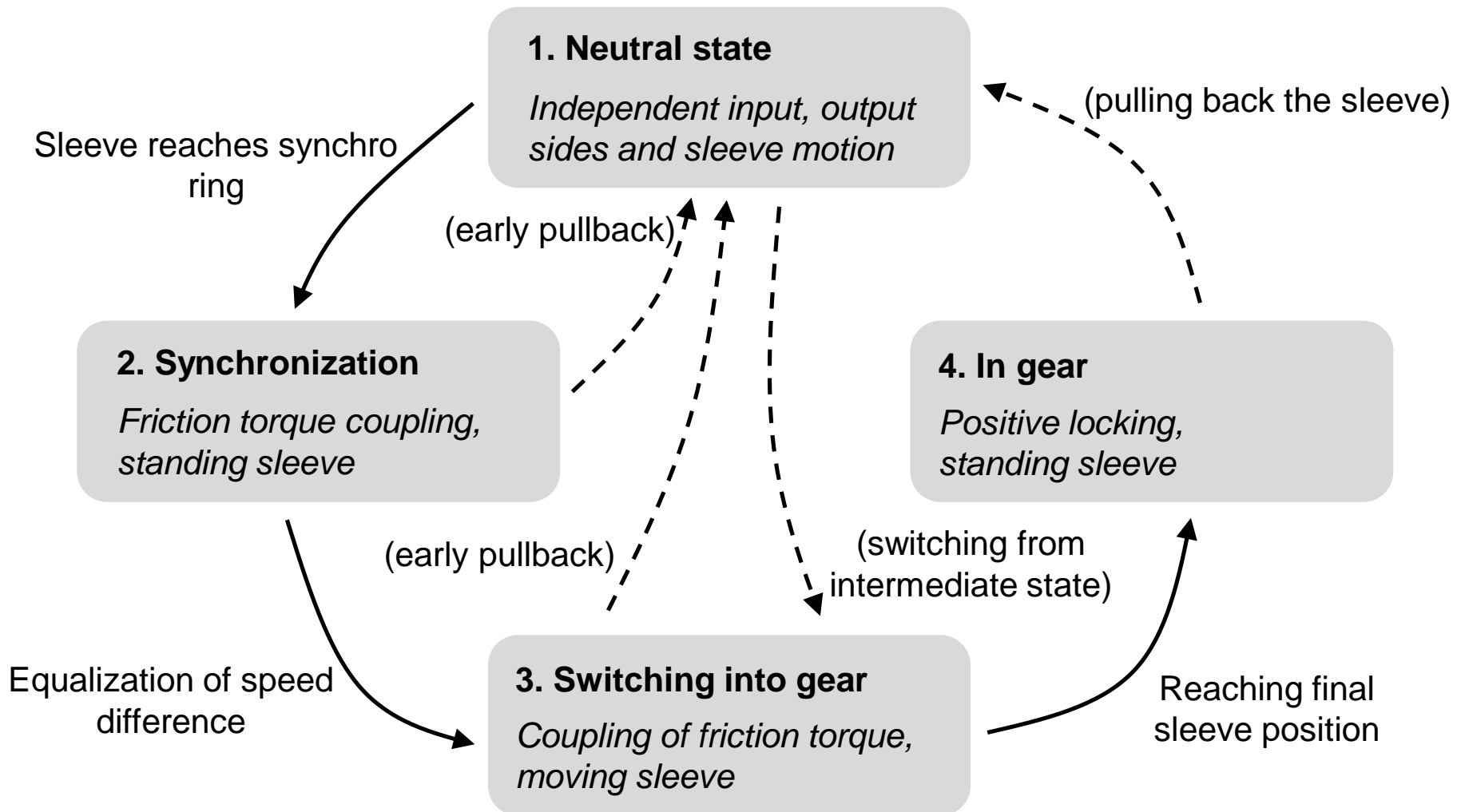
Modeled parts of the system: input reduced inertia (rotation)  
output reduced inertia (rotation)  
sleeve (progression)

Assumptions: simplified, rotationally symmetric parts  
process divided to four main parts only  
switching only from neutral position  
frictional losses neglected

Model input: axial switching force



## Definition of states and transitions of the system



## Equations of motion in state 1 (neutral position)

Equations of motion:

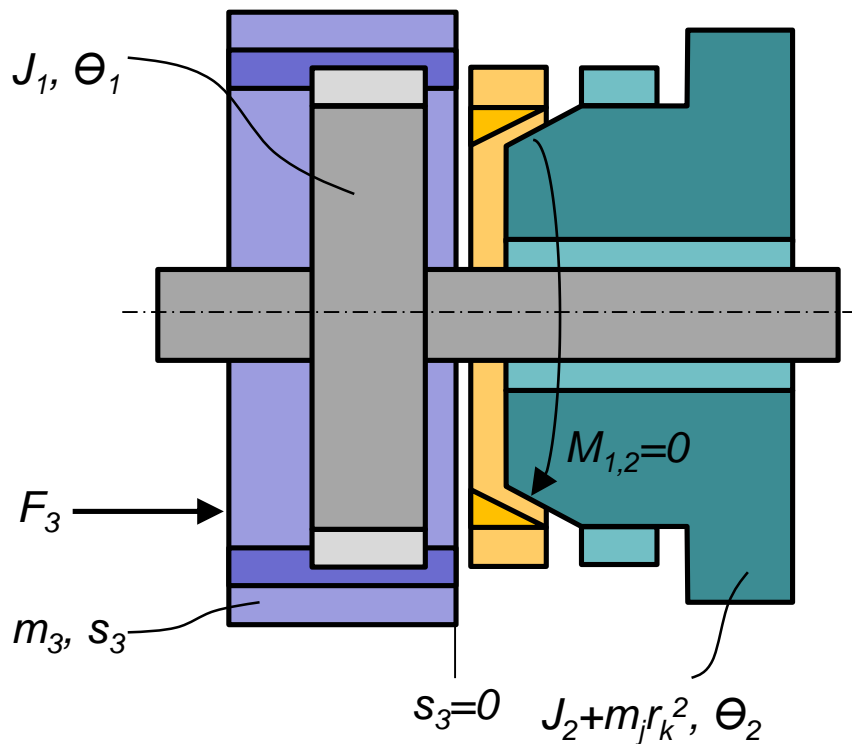
$$J_1 \ddot{\theta}_1 = M_{1,2}$$

$$(J_2 + m_j r_k^2) \ddot{\theta}_2 = -M_{1,2}$$

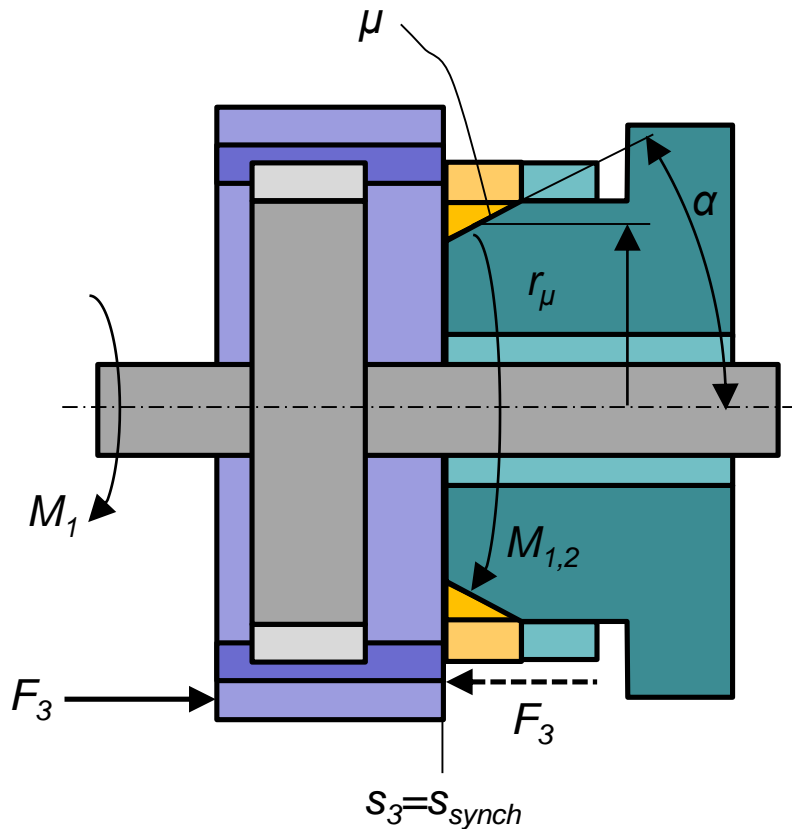
$$m_3 \ddot{s}_3 = F_3$$

Additional equations:

$$M_{1,2} = 0$$



## Equations of motion in state 2 (synchronization)



Equations of motion:

$$J_1 \ddot{\theta}_1 = M_{1,2}$$

$$(J_2 + m_j r_k^2) \ddot{\theta}_2 = -M_{1,2}$$

$$\ddot{s}_3 = 0$$

Additional equations:

$$s_3 = s_{synch} = const.$$

$$M_{1,2} = \operatorname{sgn}(\dot{\theta}_2 - \dot{\theta}_1) \frac{\mu r_\mu}{\sin \alpha} F_3$$

$$\operatorname{sgn}(u) \approx \frac{2}{1 + e^{-\sigma u}} - 1$$

## Equations of motion in state 3 (switching to gear)

Equations of motion:

$$J_1 \ddot{\theta}_1 = M_{1,2}$$

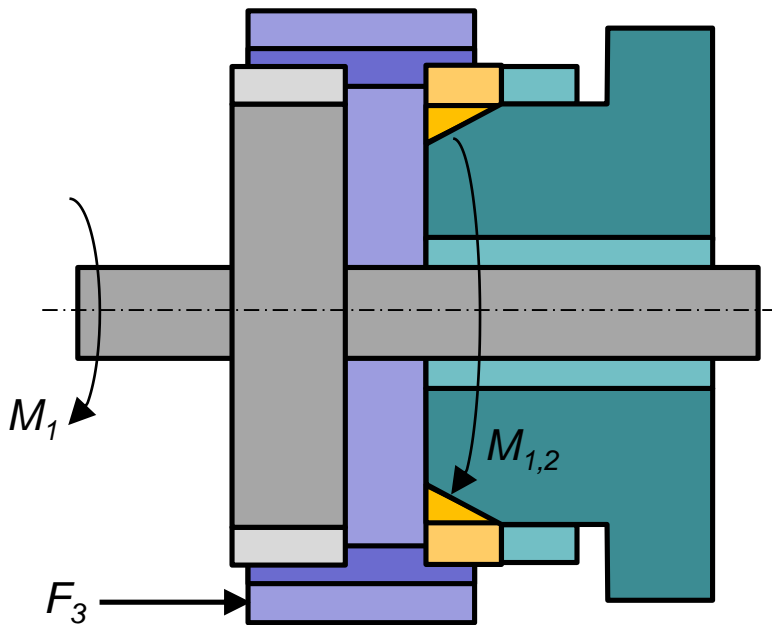
$$(J_2 + m_j r_k^2) \ddot{\theta}_2 = -M_{1,2}$$

$$m_3 \ddot{s}_3 = F_3$$

Additional equations:

$$M_{1,2} = \operatorname{sgn}(\dot{\theta}_2 - \dot{\theta}_1) \frac{\mu r_\mu}{\sin \alpha} F_3$$

$$\operatorname{sgn}(u) \approx \frac{2}{1 + e^{-\sigma u}} - 1$$



## Equations of motion in state 4 (in gear)

Equations of motion:

$$J_1 \ddot{\theta}_1 = M_{1,2}$$

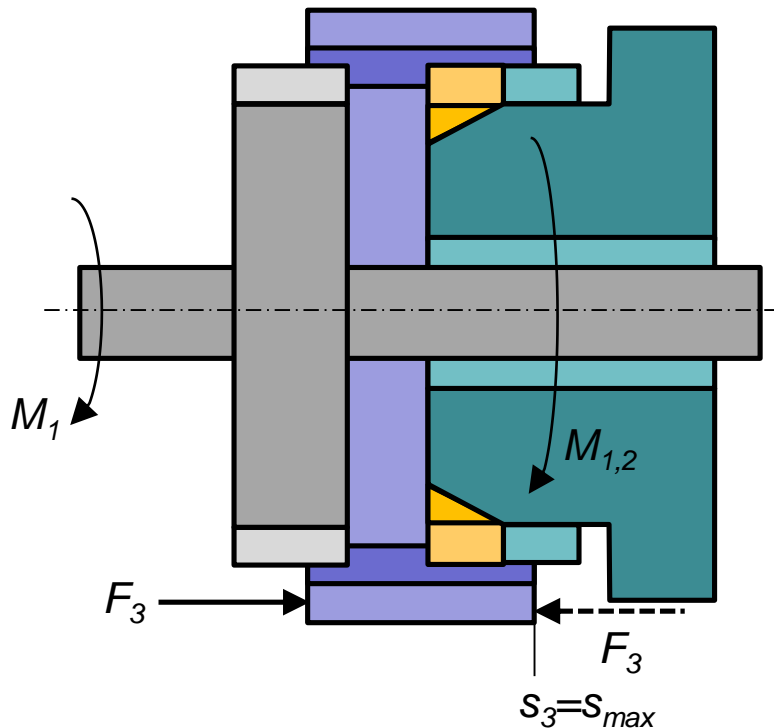
$$(J_2 + m_j r_k^2) \ddot{\theta}_2 = -M_{1,2}$$

$$\ddot{s}_3 = 0$$

Additional equations:

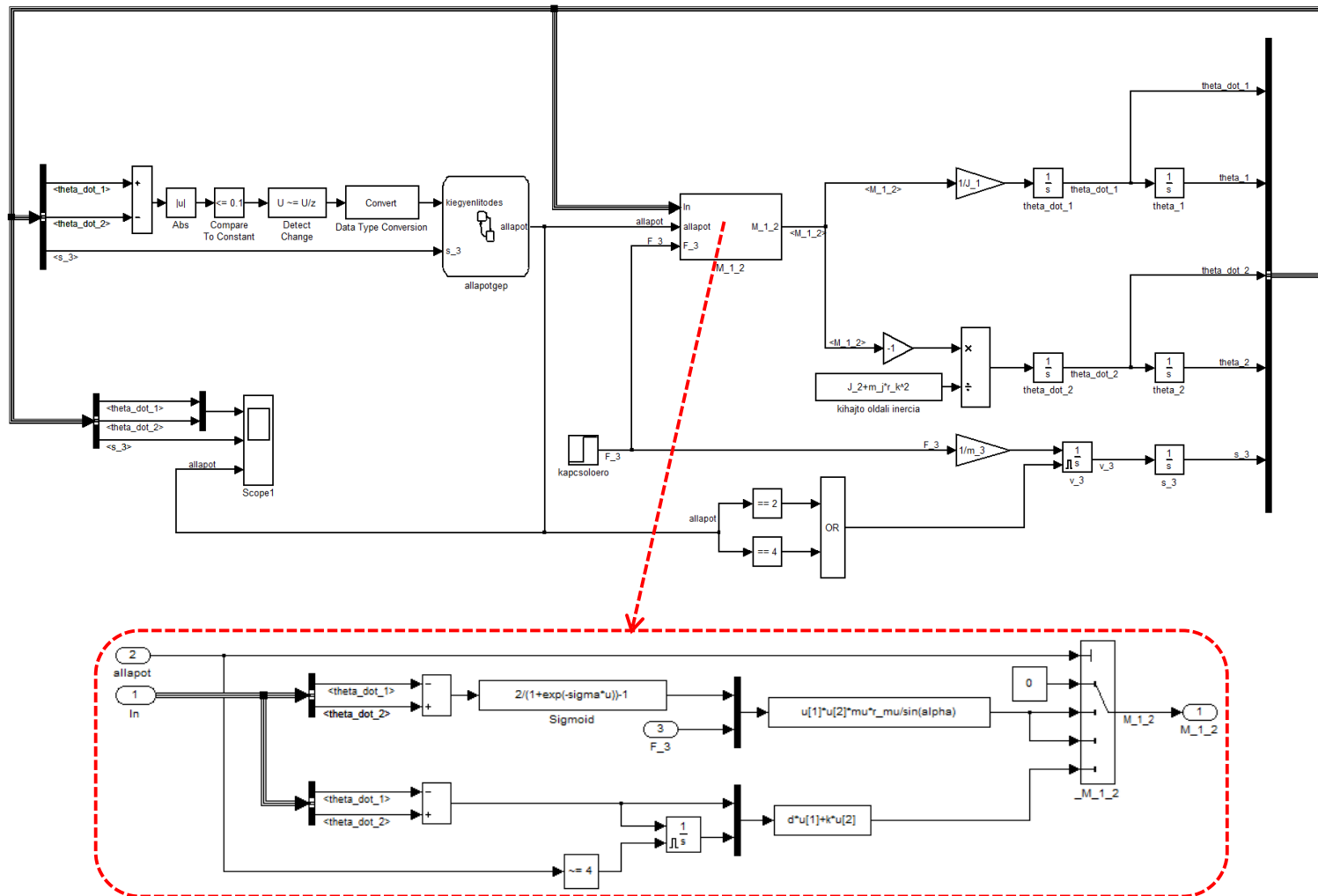
$$s_3 = s_{max} = const.$$

$$M_{1,2} = d(\dot{\theta}_2 - \dot{\theta}_1) + k \underbrace{\int (\dot{\theta}_2 - \dot{\theta}_1) dt}_{\text{Deformation-free status at the beginning of state}}$$

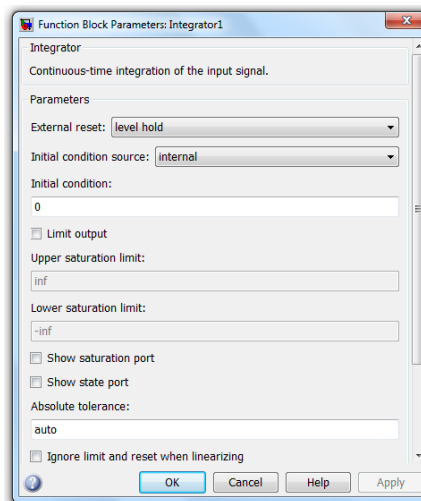
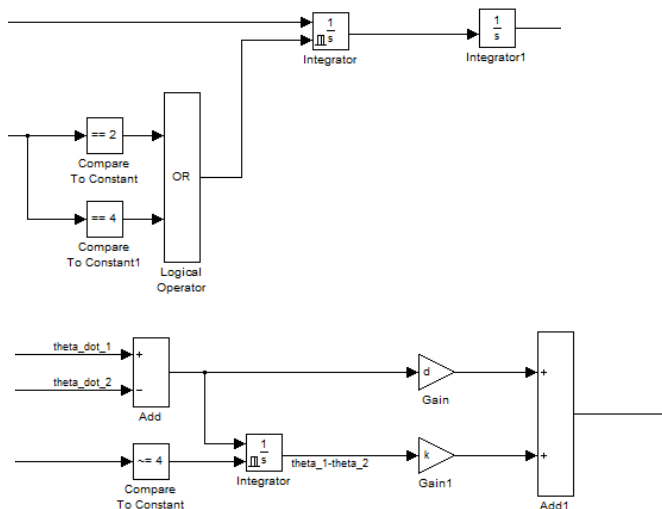


Deformation-free status at the beginning of state

## Implementation of the model in Simulink

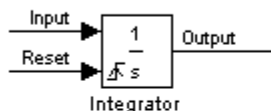


## Integrator reset



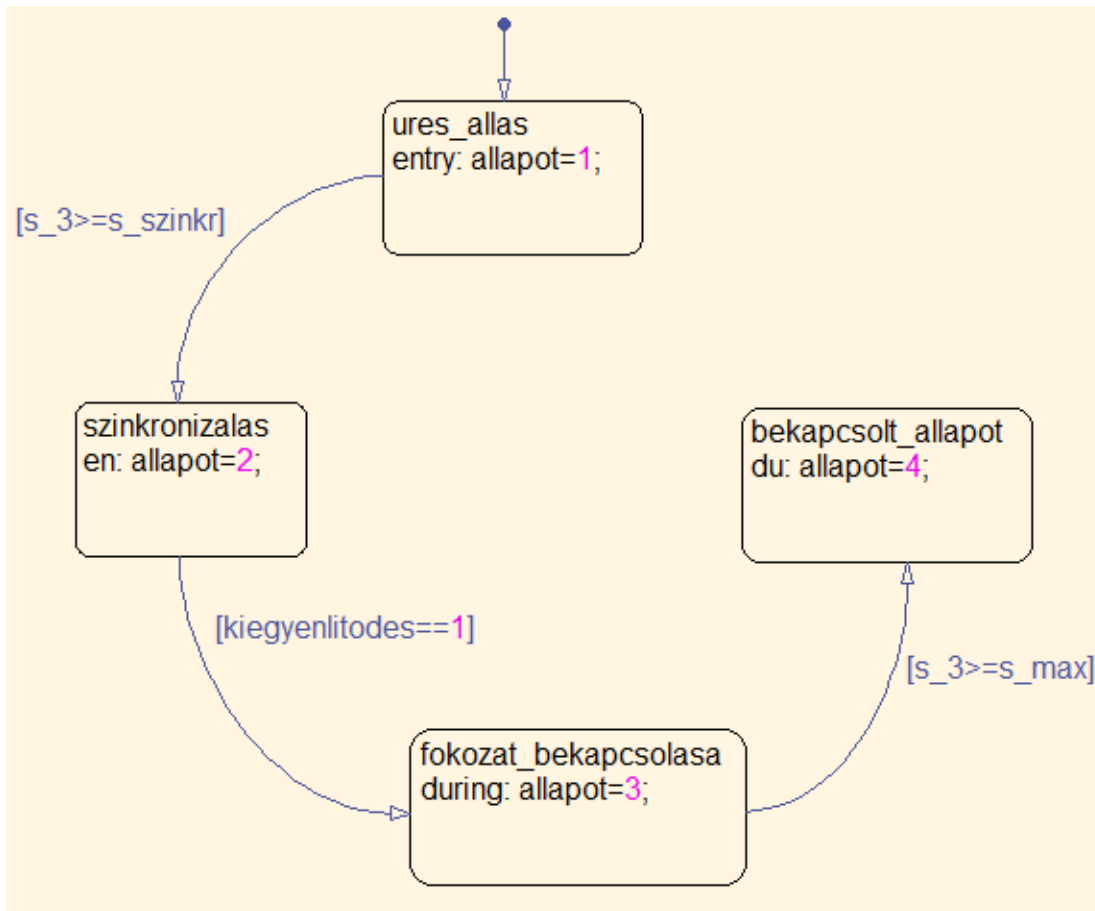
### Resetting the State

The block can reset its state to the specified initial condition based on an external signal. To cause the block to reset its state, select one of the **External reset** choices. A trigger port appears below the block's input port and indicates the trigger type.



- Select **rising** to reset the state when the reset signal rises from a zero to a positive value or from a negative to a positive value.
- Select **falling** to reset the state when the reset signal falls from a positive value to zero or from a positive to a negative value.
- Select **either** to reset the state when the reset signal changes from a zero to a nonzero value or changes sign.
- ➔ Select **level** to reset the state when the reset signal is nonzero at the current time step or changes from nonzero at the previous time step to zero at the current time step.
- ➔ Select **level hold** to reset the state when the reset signal is nonzero at the current time step.

## Implementing the state flow chart



Contents of: szinkronszerkezet/allapotgep

Name	Scope	Port	Resolve	Signal	DataType
allapot	Output	1	<input type="checkbox"/>		double
kiegyenlitodes	Input	1			double
s_3	Input	2			double
s_szinkr	Parameter				double
s_max	Parameter				double



## Model parameters

```
J_1=1;      % [kgm^2] behajtó oldali inercia
J_2=5;      % [kgm^2] kihajtó oldali inercia
m_j=1000; % [kg] járműtömeg
r_k=0.315; % [m] gördülési sugár
m_3=2;      % [kg] tolókerék tömeg

F_3=1000;   % [N] kapcsolóerő

s_szinkr=8e-3; % [m] szinkronizálási helyzet
s_max=15e-3;  % [m] max. bekapcsolt helyzet

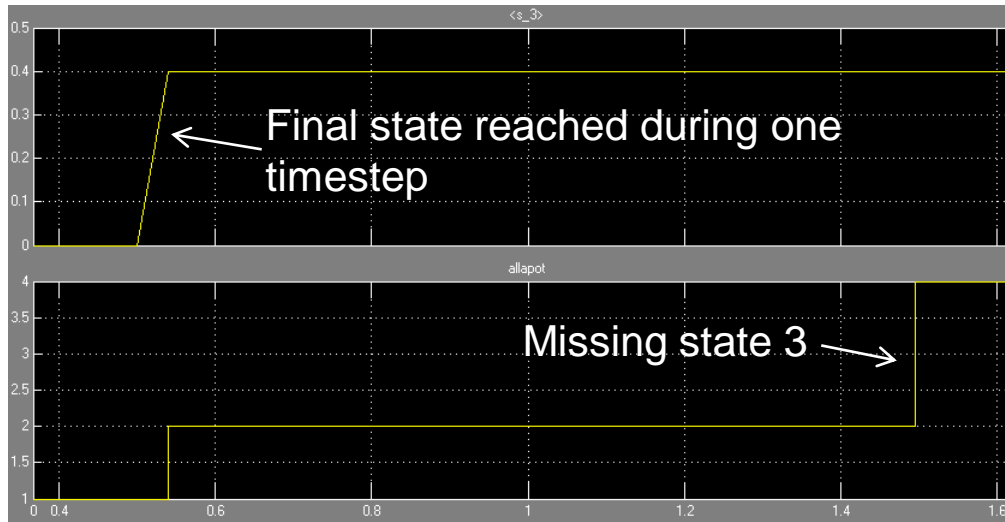
mu=0.1;      % [-] súrlódási tényező
r_mu=45e-3;  % [m] súrlódási középsugár
alpha=8*pi/180; % [rad] szinkron félkúpszög

k=1e6; % [Nm/rad] kapcsolószerkezet merevség
d=1e3; % [Nms/rad] kapcsolószerkezet csillapítás

sigma=1000; % [-] sigmoid formatényező

theta_dot_1_0=1500*2*pi/60; % [rad/s] kezdeti behajtó oldali szögsebesség
theta_dot_2_0=1000*2*pi/60; % [rad/s] kezdeti kihajtó oldali szögsebesség
s_3_0=0;          % [m] kezdeti tolókerék pozíció
```

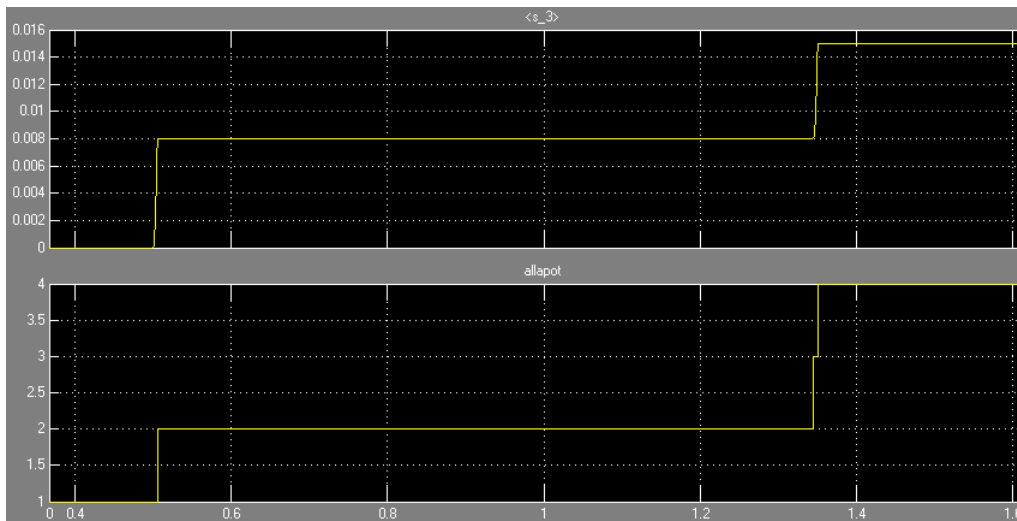
## Solver settings



Solver:

Relative tolerance:

Absolute tolerance:



Solver:

Relative tolerance:

Absolute tolerance:

Maximum order:

## References

- [1] **Lovas, L., Play, D., Márialigeti, J. and Rigal, J.-F.** Mechanical behaviour simulation for synchromesh mechanism improvements, Proc. IMechE, Part D: J. Automobile Engineering, 2006, Vol. 220, pp. 919–945 (2006)